Jordan Journal of Civil Engineering, Volume **11**, No. **2**, **2017**

Compressive Behavior of Recycled Aggregate Concrete Short Columns with Lateral Reinforcements

Heebok Choi

Associate Professor, Department of Architectural Engineering, Jeju National University, Korea.

ABSTRACT

In this study, 12 specimens with three different lateral reinforcement ratios (ρ = 0.022, 0.012 and 0.007) and four RG replacement ratios (0%, 30%, 50% and 100%) were prepared and tested under pure axial load, in order to investigate the influence of recycled coarse aggregate (RG) and lateral tie reinforcement ratio (ρ) on the compressive behavior of a confined recycled aggregate concrete (RAC) column. The results showed that the effect of RG on the compressive behavior of the RAC was negligible at low stress level and began to appear as the load increased at load levels above about 35% of the peak, regardless of ρ. The slope of the normalized compressive strength (f'_{cc} / f'_{co}) and normalized corresponding strain ($\varepsilon_{cc} / \varepsilon_{co}$) against ρ showed that the lateral reinforcement exerted the greatest effect on the stress and strain enhancement in the RG-30 series and the smallest effect in the RG-50 series. The ratios of experimental values to those predicted from Mander's model, $f'_{cc\_exp} / f'_{cc\_model}$ and $\varepsilon_{cc\_exp} / \varepsilon_{cc\_model}$ showed that the model tended to give unconservative strain (ε_{cc}) values for RAC columns. For properly estimating f'_{cc} and ε_{cc} by the existing model in case of RAC column, the main reinforced bars would be more efficient in the center of sides as well as at the corner of rectangular column section.

KEYWORDS: Recycled aggregate, Volumetric ratio of tie hoop, Compressive stress-strain behavior, Confined concrete, Rectangular column.

INTRODUCTION

The need to recycle old construction materials has been well established over the past few decades by government agencies and the construction industry due to the increasing cost of waste storage and the depletion of natural resources (Poon et al., 2007). Among the numerous construction waste materials, old concrete, in particular, is a promising source of recycled aggregate with sufficient quality for civil engineering applications with moderate performance requirements (Hansen, 1986; ACI Committee 555, 2002). While most of the studies on the subject have so far focused on the processing of old concrete and the properties of recycled aggregate concrete (RAC), only a limited number of studies have reported on the performance of structural members made of RAC beam (Han et al., 2001; Mukai and Kikuchi, 1988; Choi et al., 2010), column (Ajdukiewicz and Kliszczewicz, 2007), joint (Corinaldesi and Moricon, 2007) and frame (Xiao et al., 2006). Although a direct comparison of the results from different studies is difficult due to lack of coherent concrete constituents, the results generally indicate that the strength decreases with slight increase in the corresponding strain as recycled aggregate content in the concrete increases. This strength decrement was attributed to a weak interface between the new mortar

---

Received on 27/8/2015.
Accepted for Publication on 26/10/2016.

and the recycled aggregate and between the adhered mortar and the recycled aggregate (Poon et al., 2004; Etxeberria et al., 2006). The reduction in strength due to RG can be offset by two approaches: adjusting proportions of concrete constituents or providing proper reinforcement. The choice between the two approaches should be made based on the required structural performance and cost.

Low tensile-high compressive strength cementitious materials typically exhibit brittle behavior, but their ductility and compressive strength improve significantly when subjected to favorable biaxial pressure (Richart et al., 1928). In the past few decades, the compressive behavior of concrete confined by properly arranged lateral reinforcements has been extensively studied by many researchers (e.g., Mander et al. (1988), Koji Sakai and Sheikh (1989), Sheikh and Khoury (1997), Razvi and Saatcioglu (1999)). The effects of various parameters, including concrete strength, amount of lateral reinforcement, lateral reinforcement configuration, dimensions and cross-section geometry, on confined concrete behavior are now sufficiently understood. As a result, the use of confined concrete columns has become a common practice for seismic resistant design (ACI Committee 318, 1989). Nevertheless, as aforementioned, most of the confined concrete studies focused on concrete containing virgin aggregate. Recently, the performance of reinforced RAC frame, which satisfies the requirement set by the ACI earthquake resistant design code and the Chinese standard, has been reported by Xiao et al. (2006). Although Xiao's test demonstrated the potential use of reinforced recycled aggregate in the seismic resistance frame, few studies have investigated the effect of recycled aggregate on confined concrete members, the behavior of which is critical for modern, high performance design.

Hence, in an attempt to broaden the use of RAC, the influences of the recycled coarse aggregate (RG) content and the volumetric ratio of lateral reinforcement on the compressive behavior of confined columns subjected to concentric load are experimentally investigated here. In addition, the applicability of the existing design model (Mander et al., 1988) is assessed against the experimental results.

EXPERIMENTAL PROGRAM

Materials

River sand and crushed gravel were used as natural fine (NS) and natural coarse aggregate (NG), respectively. The recycled coarse aggregate (RG) was obtained from concrete (at least 20 years old, with a typical design compressive strength of 18 ~ 20 MPa), collected from an apartment redevelopment site in Korea. The coarse aggregates used in this study are shown in Figure (1).

Figure (1): The coarse aggregates used in this study; (a) natural coarse aggregate (NG), (b) recycled coarse aggregate (RG)

The RG was separated from the cement matrix through multiple crushing stages, while the loose fine particles were washed off the surface of the RG to minimize the effect of the fines generated during crushing (Touahamia et al., 2002). The resulting RG only contained small amounts of adhered old mortar and had similar physical properties to those of the NA, as shown in Table (1). The RG used in this study meets the Korean Industrial Standard KS F 2573 for recycled aggregate for structural concrete use. For the binder, locally manufactured, Type I Portland cement, satisfying ASTM C150 specifications, was chosen for the concrete mix.

Concrete mixes were prepared by replacing NG with RG at four different replacement ratios of 0%, 30%, 50% and 100%, as shown in Table (2). The amounts of high performance water reducing admixture (polycarboxylic acid type) and air entraining agents (neutralized vinsol resin type) were adjusted to achieve the target slump and air content of 200 mm and 6%, respectively. The average compressive strength of the control concrete was 30 ~ 34 MPa.

For each steel reinforcement bar size, three steel samples were tested under tension. The average yield strength, yield strain, Young's modulus values from the test and specified ultimate strength of the steel rebar are given in Table (3).

Table 1. Physical properties of aggregates

Type	Max. aggregate size (mm)	Specific gravity	Water absorption (%)	Fineness modulus	Bulk density (kgf/m^3)
NG	25	2.60	1.63	6.52	1642
RG		2.48	1.93	6.77	1615
NS	5	2.53	1.62	2.79	1455

Table 2. Mix proportions and wet concrete properties

Specimen	W/C (%)	S/A (%)	AD (%)	Unit Weight (N/m^3)					Slump (mm)	Air Content (%)
				W	C	NG	RG	NS		
RG-0-30	50	42	0.6	175	350	983.7	0	726.7	205	5.5
RG-0-65										
RG-0-100										
RG-30-30						688.6	301.1		200	5.0
RG-30-65										
RG-30-100										
RG-50-30						491.9	501.8		195	6.5
RG-50-65										
RG-50-100										
RG-100-30						0	1003.5		190	6.0
RG-100-65										
RG-100-100										

Table 3. Mechanical properties of deformed steel bars

Type	f_{yh}(MPa)	E_s (GPa)	ε_y ($\times 10^{-6}$)	f_{su}(MPa)
D13	420	183	2,945	630
D6	324	240	2,365	590

Column Specimens

Twelve specimens of concrete columns were prepared with three different lateral reinforcement ratios (ρ = 0.022, 0.012 and 0.007) and the aforementioned four different RG replacement ratios. The tie hoop spacing was set at 30 mm (ρ = 0.022), 65 mm (ρ = 0.012) and 100 mm (ρ = 0.007) to satisfy the minimum tie hoop spacing specified by the two standards: D/2 (100 mm), based on the earthquake-resistant design of the Architectural Institute of Korea (AIK); and D/4 (50 mm), based on the earthquake-resistant design of the ACI Committee 318-05 (ACI).

The details of the test specimens are listed in Table (4) and the detailed dimensions of the column specimens are illustrated in Figure (2). All the specimens shared the same dimensions of 200 mm × 200 mm cross-section and 600 mm height. The upper and lower 100 mm of the specimens along the length were internally reinforced with tie hoops spaced at 20 mm and fitted externally with a carbon fiber reinforced plastic wrap to prevent the bearing failure of the specimen ends prior to failure of the test area of the specimens.

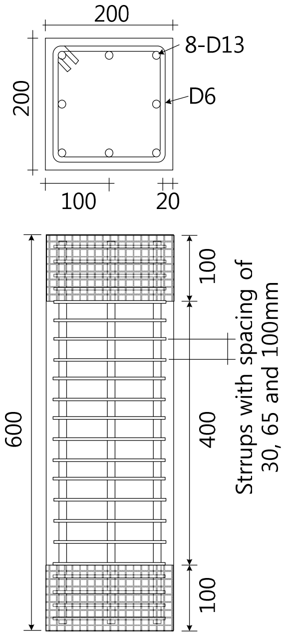

Figure (2): Specimen section and bar arrangement detail (All dimensions are in mm)

The tie hoops were made of D6 (6 mm nominal diameter) rebar and one D13 (13 mm nominal diameter) longitudinal rebar was placed at each corner of the column. The hooks of the tie hoops were anchored with 135° bending, with an extended length of 6 db, which is longer than the minimum length required by the ACI Code. The cover depth of concrete from the center of the tie hoops was 17 mm and the cross-section of the core surrounded by the center of a tie hoop was 166 mm × 166 mm. The ratio of the core area to the entire cross-section was fixed at 69% for all specimens.

Table 4. Column specimens

Specimen	Section (mm)	Tie hoop		Longitudinal rebar ratio
		Spacing	Volumetric ratio	
RG-0-30	200 X 200	30	0.012	8-D13 (0.025)
RG -0-65		65	0.006	
RG -0-100		100	0.004	
RG-30-30		30	0.012	
RG-30-65		65	0.006	
RG-30-100		100	0.004	
RG-50-30		30	0.012	
RG-50-65		65	0.006	
RG-50-100		100	0.004	
RG-100-30		30	0.012	
RG-100-65		65	0.006	
RG-100-100		100	0.004	
Type of aggregate: RG (Recycled aggregate) Replacement ratio of RGs: 0(:0%), 30(:30%), 50(:50%), 100(:100%) Tie hoop spacing: 30(:30mm), 65(:65mm), 100(:100mm)				

Test Setup and Measurement

A square plate with a semi-circular seat was placed on the top of the specimen to prevent any moment load on the specimen by eccentric load prior to application of the axial load. The loading was applied under load control such that the initial rate of displacement was about 0.30 mm/min, equivalent to 0.00075 strain/min. As load increased, the loading rate was carefully adjusted in order to trace the unloading part of the curves. The loading was stopped when the post-peak descending curve shape became apparent or when stable loading could no longer be attained. The deformation measurements were recorded at constant time intervals using a data logger (TML TDS-303). The axial deformation of the specimen was recorded from the four linear variable differential transducers (LVDTs) installed at each corner of the specimen. The average deformation value from the four LVDTs was calculated and used as the axial deformation value. It is noted here that the fixtures with vertical rigid rod with horizontal end plate placed above the LVDTs were attached to the top of the specimen in order to measure compressive deformation over the entire length of the specimen. The details of the test setup are illustrated in Figure (3).

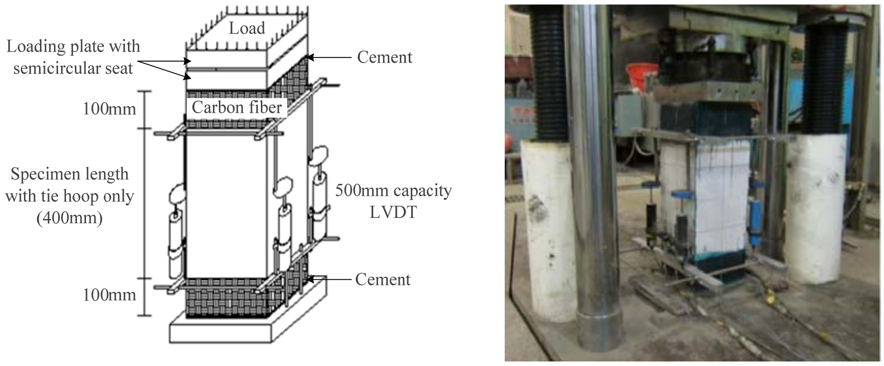

(a) Schematic illustration of loading test and specimen

(b) Photograph of loading test and specimen

Figure (3): Test set up method; (a) schematic illustration of loading test and specimen (b) photograph of loading test and specimen

RESULTS AND DISCUSSION

Failure Modes

The maximum (P_{peak}) and critical (P_{cr}) loads at which significant cover spalling occurred are listed in Table (5). Photographs of crack patterns and failure modes of the RAC column specimens after the tests are shown in Figure (4). The first visible crack appeared in vertical direction near a corner edge at 60 ~ 80% of P_{peak}, as the cover concrete deterioration worsened and P_{peak} was reached at a strain much greater than those of unconfined concretes. Subsequently, with further increase in the applied load, the cover concrete of the specimens began to spall. For a given tie hoop spacing, the rate of cover concrete spalling was proportional to the RG replacement ratio.

After localized crack damage was observed on a side of the column, notable spalling of the cover concrete occurred with a gradual decrease in the applied load. Spalling of the cover concrete occurred at a lower applied load in RAC than in natural aggregate concrete (NAC). The lower P_{cr} of RAC can be attributed to the relatively higher water absorptiveness of RG, which should have created a steeper moisture content gradient from the cover layer to the interior layer of the specimen. In turn, the moisture content gradient due to RG can cause higher incompatible drying shrinkage between the interior and exterior RAC, compared to that of NAC (Foster, 2001), thereby facilitating the cover spalling. Furthermore, the lower bond strength between the rebar and RAC than NAC (Choi and Kang, 2008) also contributes to the lower cover spalling load and the faster rate of cover degradation in RAC compared to those of NAC columns.

Figure (4): Failure modes of RAC columns

Compressive Stress-Strain Curves

Stress-strain curves of plain concrete cylinders with different RG contents up to the maximum stress are shown in Figure (5). The curves show a greater loss of stiffness at a given load level with increasing RG replacement ratio. The effect of RG on the compressive behavior of concrete became apparent at about 10 MPa, which is 31% of the average strength of the four specimens, which is similar to the result reported by Topcu and Guncan (1995).

Table 5. List of test results

Specimen	f'_{co} (MPa)	P_{cr} (kN)	ε_{cr}	P_{peak} (kN)	ε_{cc}
RG-0-30	34.1	1,190	0.00245	1816	0.00476
RG-0-65		1,110	0.00282	1712	0.00382
RG-0-100		1,086	0.00138	1675	0.00339
RG-30-30	33.5	1,150	0.00214	1815	0.00495
RG-30-65		1,050	0.00121	1638	0.00347
RG-30-100		976	0.00153	1538	0.00325
RG-50-30	32.4	1,029	0.00188	1785	0.00499
RG-50-65		1,009	0.00100	1738	0.00368
RG-50-100		882	0.00121	1677	0.00372
RG-100-30	30.5	999	0.00146	1727	0.00453
RG-100-65		985	0.00126	1622	0.00375
RG-100-100		701	0.00078	1582	0.00326

The axial compression tests of the laterally reinforced RAC columns showed that their compressive behavior in almost the entire strain range, both in the ascending and descending branches of the stress-strain curve, is affected by the RG, as shown in Figure (6). In all the specimens, the ascending branch of the stress-strain curves of the column containing RG showed a smaller increase in stress per given strain increase than that of the concrete column containing NA only and the P_{peak} value of the RAC column was lower than that of the NAC column. The lower stiffness of RAC compared to that of NAC can be attributed to the presence of microcracks in the RG and adhered mortar on the RG surface (Choi et al., 2010; Nagataki et al., 2004). At low load below 600kN (15MPa), the specimens having the same tie hoop spacing showed almost identical compressive behavior, regardless of the RG replacement ratio. However, the compressive behavior of the specimens with different RG replacement ratios began to diverge with increasing load. In the descending branch, the shape of the curves indicated that the effect of the RG content on the post-peak behavior of the column diminished by the lateral reinforcement as the ρ ratio increased. Steady curves were recorded from the RG-X-30 series which showed a gentler slope with less RG content, while curves with abrupt change in slopes were recorded from the RG-X-65 and the RG-X-100 series. In case of RG-X-30 series, the specimens showed similar ductility effects until a strain of 0.03 regardless of RG replacement ratio, but in case of RG-X-65 series, the ductility effects of RAC declined more than those of the RG-0-65 (0.016) as the minimum 0.0098 (RG-100-65) and the maximum 0.0132 (RG-30-65) with increasing RG replacement ratio. In the RG-X-100 series, the strain value of RAC declined more than that of RG-0-100 (0.095) as the minimum 0.0062 (RG-30-100) and the maximum 0.0069 (RG-50-100) and failed more quickly than RG-0-100 specimen. The steepness of the descending curves of the test specimens should correspond to the rate of concrete deterioration mentioned earlier.

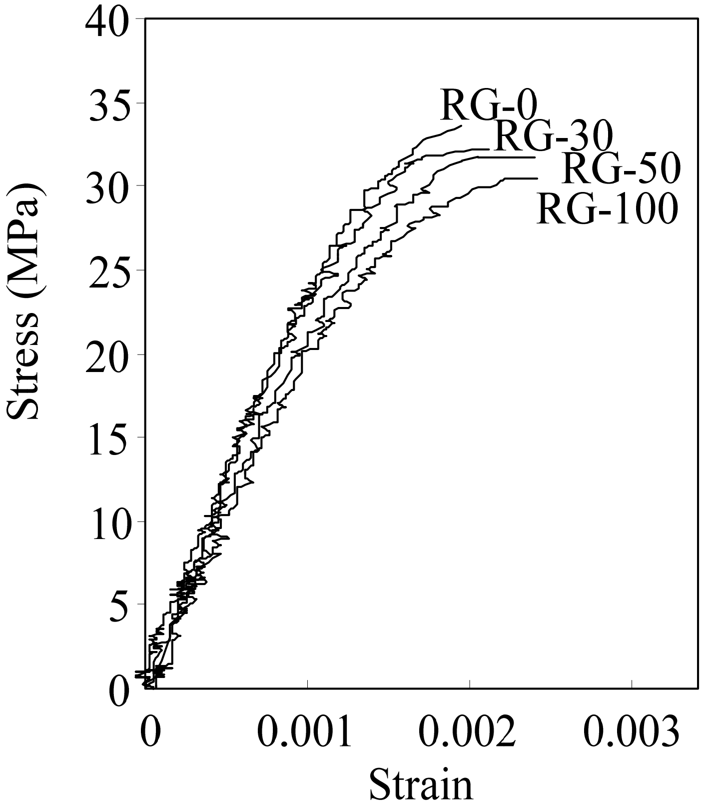

Figure (5): Stress-strain curve of unconfined concrete cylinder with different RG contents

Effect of Lateral Tie Reinforcement Ratio (ρ) on the Confined RG Concrete Strength and the Corresponding Strain

The effect of ρ on the confined RAC behavior was examined by comparing the slope of the normalized compressive strength (f'_{cc}/f'_{co}) and that of the normalized corresponding strain ($\varepsilon_{cc}/\varepsilon_{co}$) with increasing ρ. Figure (7) shows that for all four RG contents, the strength and strain enhancements of concrete were proportional to ρ. The slopes of the fitted curve in Figure (7(a)) indicate that the effect of lateral reinforcement on the strength enhancement was greatest in the RG-30 series, followed in order by RG-100, RG-0 and RG-50. Similarly, the slopes of the fitted curve in Figure (7(b)) indicate that ρ exerted the greatest effect on the strain enhancement in the RG-30 series, followed in order by RG-50, RG-0 and RG-100. Although the fitted curves of the RAC showed variations in strength and strain enhancement by lateral reinforcement from those of NAC, the confinement seemed to be effective regardless of the overall RG replacement ratio. For a fixed ρ, the strength enhancement due to the tie hoops seemed to increase with increasing RG content (at $\rho = 0.004$; $f'_{cc}/f'_{co} = 1.35$ (RG-30), $f'_{cc}/f'_{co} = 1.38$ (RG-50) and $f'_{cc}/f'_{co} = 1.42$ (RG-100)). Similarly, the strain enhancement tended to increase with increasing aggregate content (at $\rho = 0.006$; $\varepsilon_{cc}/\varepsilon_{co} = 1.48$ (RG-30), $\varepsilon_{cc}/\varepsilon_{co} = 1.53$ (RG-50) and $\varepsilon_{cc} / \varepsilon_{co} = 1.59$ (RG-100)).

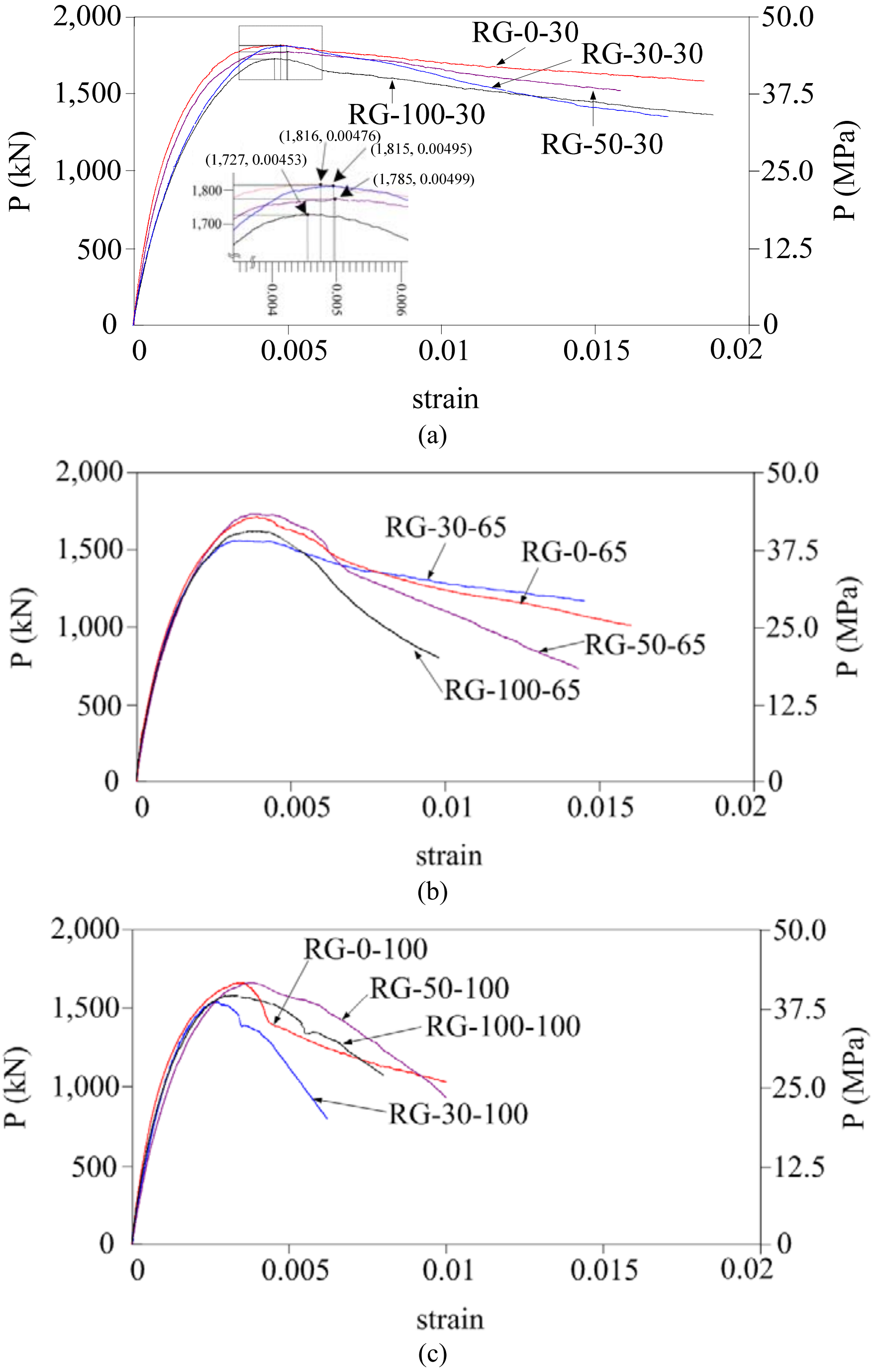

(a)

(b)

(c)

Figure (6): An axial load-strain curve of RAC column; tie hoop spacing: (a)=30 mm, (b)=65 mm and (c)=100mm

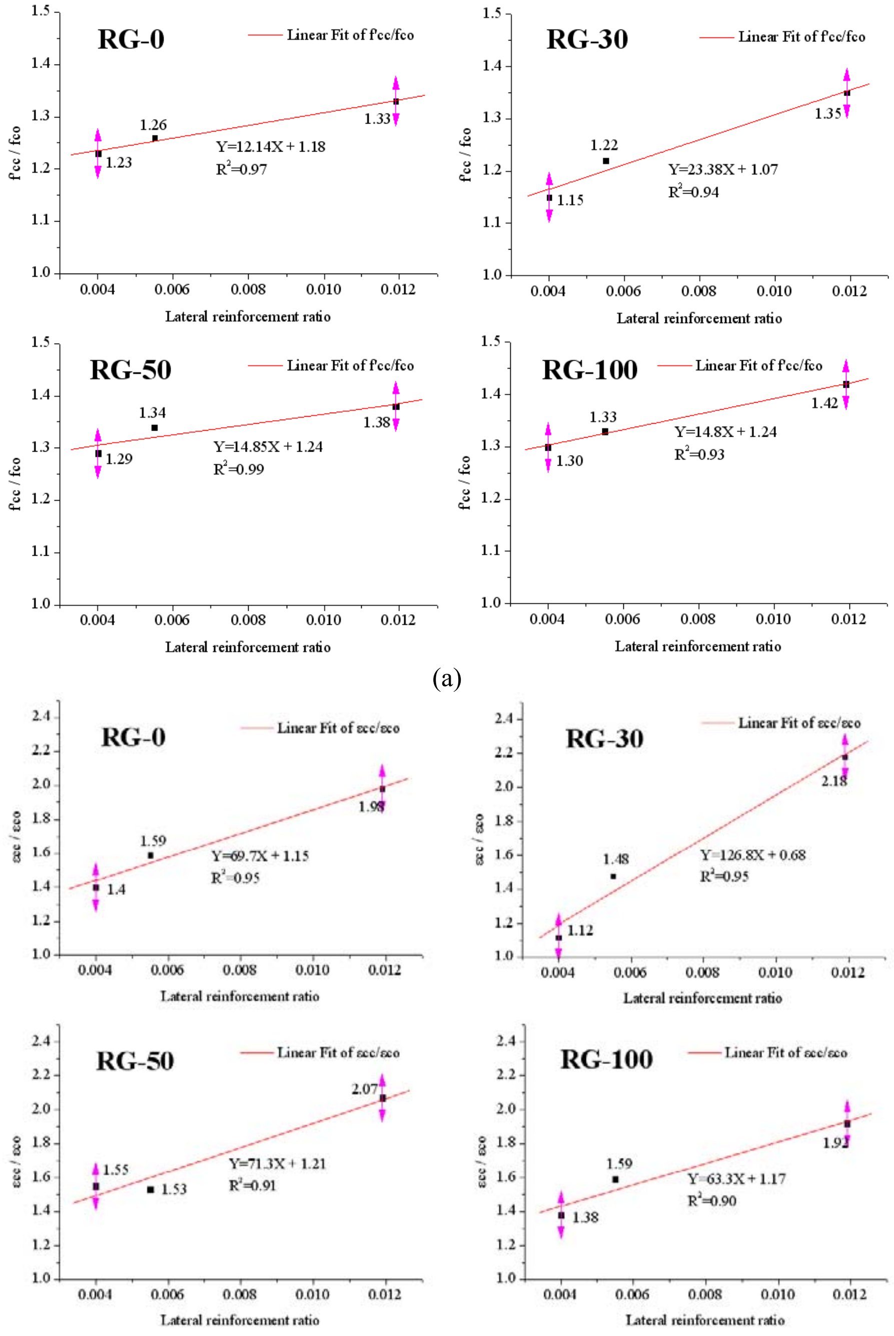

Figure (7): Effect of lateral reinforcement ratio on the enhancement of; (a) f'_{cc} and (b) ε_{cc} with different recycled aggregate contents

Comparison between Test Results and Values Predicted by the Existing Confined NAC Model

To assess the applicability of the existing compressive confined concrete model to the confined RAC, the experimental values of the confined RAC concrete's compressive strength (f'_{cc_exp}) and corresponding compressive strain (ε_{cc_exp}) at f'_{cc_exp} were compared with the values predicted by the existing model. Mander's model (Equations (1) through (3)) was selected as it is widely used in practice and research.

The confinement effectiveness coefficient (k_e) value in Equation (3) was calculated according to the method suggested for rectangular concrete sections confined by rectangular hoops with or without cross tie by Mander et al. (1988(b)).

$$f'_{cc} = f'_{co}\left(2.254\sqrt{1+\frac{7.94\cdot f'_l}{f'_{co}}} - \frac{2\cdot f'_l}{f'_{co}} - 1.254\right) \tag{1}$$

$$\varepsilon_{cc} = \varepsilon_{co}\left[1+5\left(\frac{f'_{cc}}{f'_{co}}-1\right)\right] \tag{2}$$

$$f'_l = k_e \rho f_{yh} \tag{3}$$

where f'_{co}= compressive strength of unconfined concrete; ε_{co} = compressive strain of unconfined concrete at f'_{co}; f'_{cc} = compressive strength of confined concrete; ε_{cc} = compressive strain of confined concrete at f'_{cc} ; f_{yh} = yield strength of lateral reinforcement; k_e = confinement effectiveness coefficient; ρ=volumetric ratio of transverse steel reinforcement.

The ratios of the experimental values to those predicted from the existing model, $f'_{cc\_exp}/f'_{cc\_model}$ and $\varepsilon_{cc\_exp}/\varepsilon_{cc\_model}$, are shown in Table (6). The average $f'_{cc\_exp}/f'_{cc\_model}$ and $\varepsilon_{cc\_exp}/\varepsilon_{cc\_model}$ were 0.98 and 0.79, with standard deviations of 0.069 and 0.065, respectively. These results indicate that the existing Mander's model gave unconservative strain (ε_{cc}) values for the RAC columns. This may be explained by the fact that as Mander's model was originally developed to predict the confined strength and corresponding strain of normal concrete made of natural aggregates, it therefore does not account for different RG replacement ratios in conjunction with different ρ. The discrepancy observed between the predicted and experimental values is in agreement with Van Mier (1986) and Shah and Ahmad (1994), who stated that it is not sufficient to determine the mechanical behavior of confined concrete by parameters, such as concrete strength, yield strength and volumetric ratio of the confining reinforcement. The importance of aggregate type was also reported by El-Dash and Ramadan (2006), who found that the aggregate type influences the behavior of confined concrete, especially the roundness of the aggregate, which assists to distribute the lateral confinement pressure and helps the concrete element resist higher stress than angular aggregate. Therefore, as well as the parameters noted above, the type of aggregate and its content shall also be considered in the model.

Table 6. Comparison of experiment results to existing model

Specimen	**Confined strength f'_{cc} (MPa)**			**Confined strain ε_{cc} (MPa)**		
	Exp.	Model	Exp./ Model	Exp.	Model	Exp./ Model
RG-0-30	45.40	43.764	1.04	0.00476	0.0063765	0.75
RG-0-65	42.80	38.757	1.10	0.00382	0.0054616	0.70
RG-0-100	41.88	37.203	1.13	0.00339	0.0051361	0.66
RG-30-30	45.38	43.148	1.05	0.00495	0.0062933	0.79
RG-30-65	40.95	38.153	1.07	0.00337	0.0047941	0.70
RG-30-100	38.45	36.601	1.05	0.00255	0.0039471	0.65
RG-50-30	44.63	42.017	1.06	0.00499	0.0069278	0.72
RG-50-65	43.45	37.046	1.17	0.00368	0.0064926	0.57
RG-50-100	41.93	35.497	1.18	0.00372	0.0059278	0.63
RG-100-30	43.18	40.059	1.08	0.00453	0.007233	0.63
RG-100-65	40.55	35.131	1.15	0.00375	0.0062217	0.60
RG-100-100	39.55	33.591	1.18	0.00326	0.0058365	0.56

Figure (8) shows that the existing model reasonably estimates the compressive strength and strain of the RAC columns with the lateral reinforcement about bar arrangement shape (Wi') of this experiment and normal bar arrangement shape (Wi). The average ratio of $f'_{cc\_exp}/f'_{cc\_model}$ in the bar arrangement shape (Wi') was nearer to 1 than that of normal bar arrangement shape (Wi) for hoop spacing of 30 mm. But, for hoop spacings of 65 mm and 100 mm, the average ratio of $f'_{cc\_exp}/f'_{cc\_model}$ in the bar arrangement shape (Wi') was underestimated by the existing model. $\varepsilon_{cc\_exp}/\varepsilon_{cc\_model}$ ratio by the existing model, in the bar arrangement shape (Wi'), was estimated more effectively than that of normal bar arrangement shape (Wi) for the tie hoop spacings of 30 mm, 65 mm and 100 mm. In other words, in RAC columns, f'_{cc} by the existing model was properly estimated and ε_{cc} was overestimated in narrow tie hoop spacing. And for properly estimating f'_{cc} and ε_{cc} by the existing model in case of RAC columns, the main reinforced bars would be more efficient in the center of sides as well as at the corner of rectangular column section.

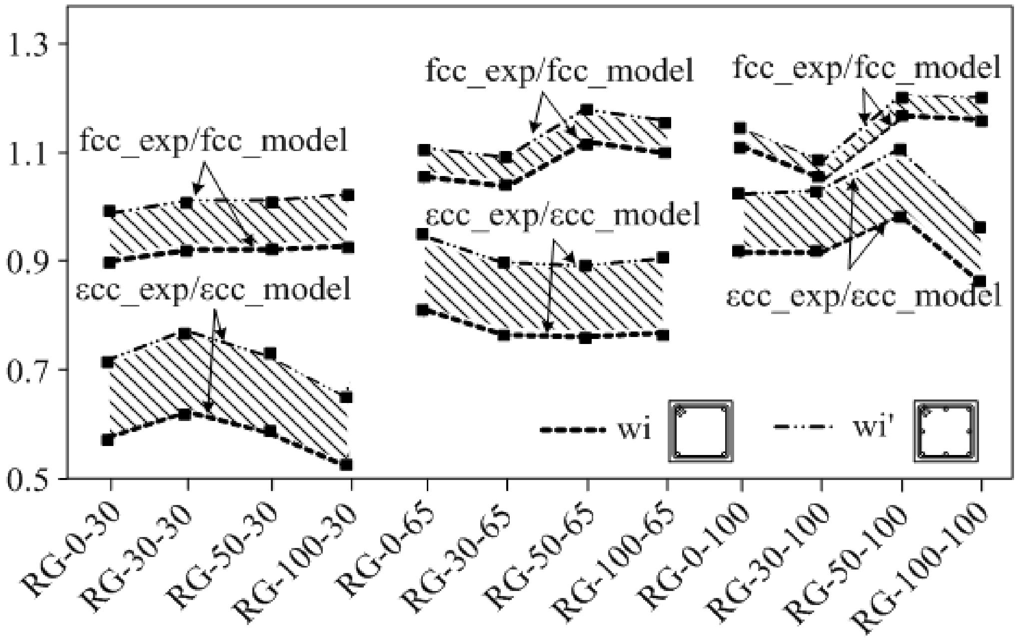

Figure (8): Comparison between experimental values and those predicted by the existing Mander's model

CONCLUSIONS

Based on the results of the RAC compressive test and comparison between the test results and the values predicted by the existing model, the following conclusions were drawn:

(1) The effect of RG on the compressive confined RAC column was negligible in the ascending branch of the load-strain curve up to 600 kN, which was about 35% of the average confined strength of all specimens tested.

(2) Examination of the stress-strain curves indicated that the influence of the RG content increased in both the ascending and descending branches of the stress-strain curves with decreasing ρ.

(3) The average $f'_{cc\_exp}/f'_{cc\_model}$ and $\varepsilon_{cc\_exp}/\varepsilon_{cc\_model}$ were 0.98 and 0.79, with standard deviations of 0.069 and 0.065, respectively. These results indicated that the existing Mander's model gave unconservative strain (ε_{cc}) values for the RAC columns.

(4) In RAC columns, f'_{cc} by the existing model was properly estimated and ε_{cc} was overestimated in narrow tie hoop spacing. And for properly estimating f'_{cc} and ε_{cc} by the existing model in case of RAC columns, the main reinforced bars would be more efficient in the center of sides as well as at the corner of rectangular column section.

Nomenclature

f_{yh} =Yield strength of lateral reinforcement [MPa]

E_s= Young's modulus of reinforcement [GPa]

f_{su}= Tensile strength of reinforcement [MPa]

ε_y=Yield strain of reinforcement

P_{cr}= Load at onset of first visible cracking [kN]

ε_{cr}=Strain at onset of first visible cracking

P_{peak}= Maximum applied compressive load [kN]

f'_{co} = Compressive strength of unconfined concrete containing specified recycled aggregate content [MPa]

ε_{co}= Compressive strain of unconfined concrete at f'_{co}

f'_{cc} = Compressive strength of confined concrete [MPa]

ε_{cc} = Compressive strain of confined concrete at f'_{cc}

A_s = Area of tie hoop bar

D' = Nominal diameter of tie hoop bar

k_e = confinement effectiveness coefficient

ρ=volumetric ratio of transverse steel reinforcement

γ=RG replacement ratio (%)

REFERENCES

ACI Committee 318. (1989). "Building code requirements for reinforced concrete and commentary (ACI 319-89, ACI319R-89)". American Concrete Institute, Detroit, Mich.

ACI Committee 318. (2005). "Building code requirements for structural concrete (ACI 318-05) and commentary (ACI 318R-05)". American Concrete Institute, Farmington Hills, Mich., 430 p.

ACI Committee 555. (2002). "Removal and reuse of hardened concrete". ACI Materials Journal, 99 (3), 300-325.

Ajdukiewicz, Andrzej B., and Kliszczewicz, Alina T. (2007). "Comparative tests of beams and columns made of recycled aggregate concrete and natural aggregate concrete." Journal of Advanced Concrete Technology, l5 (2), 259-273.

Choi, H.B. (2010). "Recycled aggregate-paste interaction mechanism by micro-structure analysis." PhD Thesis, Korea University, Seoul, Korea.

Choi, H.B., and Kang, K.I. (2008). "Bond behaviour of deformed bars embedded in RAC." Magazine of Concrete Research, 60 (6), 399-410.

Choi, H.B., Yi, H.H., and Kang, K.I. (2010). "Experimental study on the shear strength of recycled aggregate concrete beams." Magazine of Concrete Research, 62 (2), 103-114.

Etxeberria, M., Vázquez, E., and Marí, A. (2006). "Microstructure analysis of hardened recycled aggregate concrete." Magazine of Concrete Research, 58 (10), 683-690.

Foster, Stephen J. (2001). "On the behavior of high-strength concrete columns: cover spalling, steel fibers and ductility". ACI Structural Journal, 98 (4), 583-589.

Han, B.C., Yun, H.D., and Chung, S.Y. (2001). "Shear capacity of reinforced concrete beams made with recycled aggregate." ACI Special Publication, 200 (31), 503-515.

Hansen, T.C. (1986). "Recycled aggregate and recycled aggregate concrete 2nd state-of-art report development from 1945-1985." Materials and Structures, 19 (3), 201-246.

Jianzhuan Xiao, Yuedong Sun, and H. Falkner. (2006). "Seismic performance of frame structures with recycled aggregate concrete." Engineering Structures, 28 (1), 1-8.

Karim, M. El-Dash, and Mohamed, Ramadan O. (2006). "Effect of aggregate on the performance of confined concrete." Cement and Concrete Research, 36 (3), 599-605.

Koji Sakai, and Shamim A. Sheikh. (1989). "What do we know about confinement in reinforced concrete columns?." ACI Structure Journal, 86 (2), 192-207.

Mander, J.B., Priestley, M.J.N., and Park, R. (1984). "Seismic design of bridge piers." Res. Rep. 84-2, Dept. of Civ. Engrg., Univ. of Canterbury, Christchurch, New Zealand.

Mander, J.B., Priestley, M.J.N., and Park, R. (1988(a)). "Observed stress-strain behavior of confined concrete." ASCE Journal of Structural Engineering, 114 (8), 1827-1849.

Mander, J.B., Priestley, M.J.N., and Park, R. (1988(b)). "Theoretical stress-strain model for confined concrete." ASCE Journal of Structural Engineering, 114 (8), 1804-1826.

Mukai, T., and Kikuchi, M. (1988). "Properties of reinforced concrete beams containing recycled aggregate." In: Y. Kasai, Editor, Proceedings of 2nd International RILEM Symposium on Demolition and Reuse of Concrete and Masonry, Tokyo, 2, 670-679.

Nagataki, S., Gokce, A., Saeki, A., and Hisada, M. (2004). "Assessment of recycling process induced damage sensitivity of recycled aggregate concrete aggregates." Cement and Concrete Research, 34 (6), 965-971.

Poon, C.S., and Chan, D. (2007). "The use of recycled aggregate in concrete in Hong Kong." Resources Conservation and Recycling, 50 (3), 293–305.

Poon, C.S., Shui, Z.H., and Lam, L. (2004). "Effect of microstructure of ITZ on compressive strength of concrete with recycled aggregates." Construction and Building Materials, 18 (6), 461-468.

Richart, F.E., Brandtzeag, A., and Brown, R.L. (1928). "A study of the failure of concrete under combined compressive strength". Bulletin 185, Univ. of Illinois Engineering Experimental Station, Champaign, III.

Salim Razvi, and Murat Saatcioglu. (1999). "Confinement model for high-strength concrete". ASCE Journal of Structural Engineering, 125 (3), 281-289.

Shah, S.P., and Ahmad, S.H. (1994). "High-performance concrete: properties and applications". McGraw-Hill, Inc.

Sheikh, Shamim A., and Shafik S. Khoury. (1997). "A performance-based approach for the design of confining steel in tied column." ACI Structural Journal, 94 (4), 421-431.

Sheikh, Shamim A., and Yeh, C.C. (1986). "Flexural behavior of confined concrete columns". ACI Journal Proceedings, 83 (3), 389-404.

Topcu, I.B., and Guncan, N.F. (1995). "Using waste concrete as aggregate." Cement and Concrete Research, 25 (7), 1385-1390.

Touahamia, M., Sivakumar, V., and McKelvey, D. (2002). "Shear strength of reinforced-recycled material." Construction and Building Materials, 16 (6), 331-339.

Valeria Corinaldesi, and Giacomo Moricon. (2006). "Behavior of beam-column joints made of sustainable concrete under cyclic loading". J. Mat. in Civ. Eng., 18 (5), 650-658.

Van Mier, J.G.M. (1986). "Fracture of concrete under complex stress". Heron, Delft University of Technology, Netherlands.